Frequency-dependent conductivity in sputtered amorphous phosphorus thin films

P. Extance*
Cavendish Laboratory, University of Cambridge, Madingley Road, Cambridge, United Kingdom CB3 0HE

S. R. Elliott
Department of Physical Chemistry, University of Cambridge, Lensfield Road, Cambridge, United Kingdom CB2 1EP

E. A. Davis†
Cavendish Laboratory, University of Cambridge, Madingley Road, Cambridge, United Kingdom CB3 0HE
(Received 25 October 1984)

The first measurements are reported of frequency-dependent (ac) conductivity in thin films of amorphous phosphorus prepared by rf sputtering. The behavior of the ac conductivity $\sigma(\omega)$ is broadly similar to that which has been observed previously in many other types of amorphous semiconductors, namely a nearly linear frequency dependence but a weak temperature dependence. However, there are subtle but important differences for films treated in different ways. As-deposited films show a relatively large temperature dependence of $\sigma(\omega)$ and of its frequency exponent s: annealing, or hydrogenation during the sputtering deposition, acts to decrease the temperature dependences of both quantities. The results are analyzed with reference to three models of the ac conductivity in amorphous semiconductors. It is shown that the best agreement is with the correlated barrier hopping model of ac conductivity and it is concluded that paramagnetic, neutral dangling-bond defects (D^0) predominate in the ac loss process in the as-deposited material, whereas diamagnetic, charged defects (D^+,D^-) predominate in annealed films.

I. INTRODUCTION

A frequency-dependent (ac) electrical conductivity $\sigma_{ac}(\omega)$ has been observed in very many amorphous semiconductors and insulators (both inorganic and polymeric organic materials), and invariably has the form

$$\sigma_{ac}(\omega)=A\omega^s , \tag{1}$$

where ω is the (circular) frequency and the exponent s is less than or equal to unity. Indeed, so widespread is this phenomenon that it appears to be a universal feature of the amorphous nonmetallic state. In fact, all that is required to give this behavior is that the loss mechanism should have a very wide range of possible relaxation times τ; in particular, a nearly linear frequency dependence of $\sigma(\omega)$ is predicted if the distribution of relaxation times, $n(\tau)$, is inversely proportional to τ, which results if τ is an exponential function of a random variable ζ, $\tau=\tau_0\exp(\zeta)$ (where τ_0 is a characteristic relaxation time, often taken to be an inverse phonon frequency, ν_{ph}^{-1}), with any departures from linearity carrying information on the particular type of loss mechanism involved (see, e.g., Refs. 1 and 2). It should be noted that what is measured in a given experiment is the *total* conductivity $\sigma_{tot}(\omega)$ of the sample at the particular frequency and temperature. In general, this can be written as

$$\sigma_{tot}(\omega)=\sigma_{ac}(\omega)+\sigma_{dc} , \tag{2}$$

where σ_{dc} is the dc conductivity, and it is tacitly assumed that the ac and dc conductivities are due to *completely different* processes. Examples of this separation might be when $\sigma(\omega)$ is due to hopping between defect centers and σ_{dc} is due to band conduction in extended states; alternatively, if *both* processes are due to hopping between localized states, then $\sigma_{ac}(\omega)$ could arise solely (or predominantly) from carrier motion within isolated regions (e.g., voids), whereas σ_{dc} could result from percolation channels established throughout the sample. If these conditions are not met, and σ_{dc} is simply the $\omega\rightarrow 0$ limit of $\sigma_{ac}(\omega)$, then the separation as given in Eq. (2) is no longer useful.

Many different theories for ac conduction in amorphous semiconductors have been proposed in the past, and the interested reader is referred to the extensive reviews on this subject[2,3] for details. It is commonly assumed that the "pair approximation" holds; namely, the dielectric loss occurs because carrier motion is considered to be localized within pairs of sites; this is the high-frequency limit of the general case where multiple hopping can occur between a number of centers in a cluster. In essence, two distinct processes have been proposed for the relaxation mechanism, namely quantum-mechanical tunneling (QMT) or classical hopping over a barrier (or some combination or variant of the two) and it has been variously assumed that electrons or atoms (carrying at least some charge) are the carriers responsible.

To compare the various models with the experimental data for a-P, the detailed predictions of the temperature and frequency dependence need to be examined, and thus each approach is discussed in some detail below.

For the QMT model the random variable is $\zeta=2\alpha R$, where R is the intersite separation and α^{-1} is the spatial decay parameter for the s-like wave function assumed to describe the localized state at each site; it is assumed com-

monly that α is constant for all sites. Numerous authors[3–8] have evaluated within the pair approximation the ac conductivity for single-electron motion undergoing QMT, obtaining the expression

$$\sigma_{ac}(\omega)=\frac{Ce^2g_0^2kT}{\alpha}\omega R_\omega^4 , \tag{3}$$

where C is a numerical constant which varies slightly according to different authors, but may be taken to be $\pi^4/24$ (see Refs. 3, 6, and 8), g_0 is the (assumed constant) density of states (in $eV^{-1}cm^{-3}$) within which conduction takes place ($=N/\Delta_0$, where N is the spatial density of states and Δ_0 is the bandwidth), and the hopping distance at a particular frequency, R_ω, is given by

$$R_\omega=\frac{1}{2\alpha}\ln(1/\omega\tau_0) , \tag{4}$$

where $\ln(1/\omega\tau_0)$ is a positive quantity.

The frequency dependence of such an expression for $\sigma_{ac}(\omega)$ [i.e., in the form of Eq. (1)] can be deduced using the relation

$$s=\frac{d\{\ln[\sigma_{ac}(\omega)]\}}{d(\ln\omega)} , \tag{5}$$

and for the QMT model [Eq. (3)], this gives

$$s=1-\frac{4}{\ln(1/\omega\tau_0)} . \tag{6}$$

[Note that the above results are obtained in the wide-band case (i.e., for $\Delta_0 \gg kT$).] Thus, the QMT model predicts that the frequency exponent s of $\sigma(\omega)$ is temperature independent, but frequency dependent, and, for typical values of the parameters involved in Eq. (6), namely $\tau_0 \simeq 10^{-13}$ s and $\omega \simeq 10^4$ s^{-1}, a value of $s \simeq 0.81$ is deduced.

A temperature-dependent frequency exponent *can* be obtained within the framework of the QMT model (in the pair approximation) by assuming that the carriers form nonoverlapping small polarons, i.e., the total energy of a charge carrier is lowered by the polaron energy W_p (assumed to be constant for all sites), resulting from the lattice distortion accompanying the occupation of a site by a carrier. Transfer of an electron between degenerate sites having a random distribution of separations will therefore generally involve an activation energy, the polaron hopping energy $W_H \simeq W_p/2$. In this case, the frequency exponent of $\sigma(\omega)$ becomes

$$s=1-\frac{4}{\ln(1/\omega\tau_0)-W_H/kT} , \tag{7}$$

Note that now s is temperature dependent, increasing with increasing temperature (see Fig. 1). It should also be noted that a temperature-dependent frequency exponent *can* arise from the simple QMT model if the pair approximation breaks down, i.e., when the carrier motion occurs within clusters rather than being confined to pairs of sites.[9]

The behavior of the nonoverlapping-small-polaron model might, at first sight, appear to be pathological in that inspection of Eq. (7) shows the frequency exponent s can apparently become infinite at sufficiently high frequencies and/or low temperatures. This nonphysical behavior is caused by the hopping length,

$$R_\omega=(2\alpha)^{-1}[\ln(1/\omega\tau_0)-W_H/kT]$$

tending to zero when the term in square brackets tends to zero.[2] In practice, of course, the minimum value of R_ω is equal to the interatomic spacing; for higher frequencies or lower temperatures than given by the critical condition, the contribution to the overall ac conductivity due to the small-polaron tunneling mechanism would tend to zero.

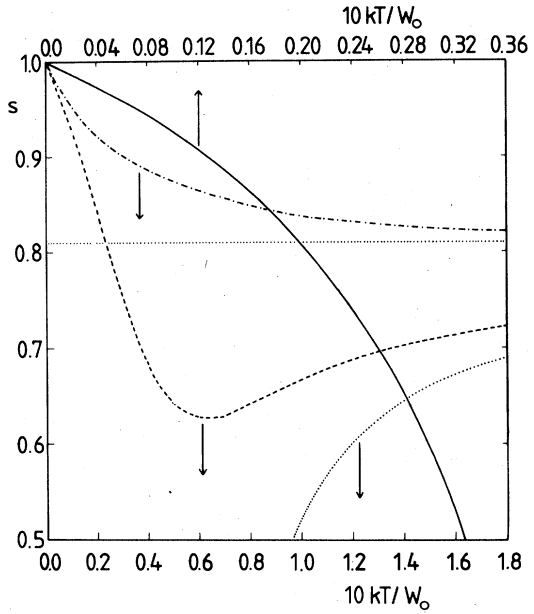

FIG. 1. Temperature dependence of the frequency exponent s of the ac conductivity predicted by various models and plotted versus reduced temperature kT/W_0. The solid curve is for the correlated-barrier-hopping (CBH) model; the dashed and dashed-dotted curves refer to the overlapping-large-polaron (OPW) model, with values for the normalized polaron radius of $r_0'=2.5$ and 20, respectively; the dotted curve refers to the quantum-mechanical tunneling (QMT) model with nonoverlapping (small) polarons; the horizontal dotted line refers to the simple QMT model. Note the difference in the upper and lower reduced temperature scales. W_0 in the upper scale is equal to W_M, and in the lower scale is equal to W_{H0}.

The other type of process which has been proposed for the relaxation mechanism is classical hopping over a barrier (HOB), where the random variable is $\zeta=W/kT$. For the case of *atomic* motion, the following expression is obtained[10] (also see Ref. 3):

$$\sigma(\omega)=\frac{\pi}{3}\eta\frac{Np^2kT}{W_0\Delta_0}\tanh\left[\frac{\Delta_0}{2kT}\right]\omega , \tag{8}$$

where η is a mean-field correction term, N is the number of pair states per unit volume, p is the dipole moment associated with the transition, and it is assumed that the energy difference between sites, Δ, is randomly distributed in the range $0<\Delta<\Delta_0$ and the barrier height is also ran-

domly distributed in the range $0<W<W_0$. Note from Eq. (8) that, for the case of simple HOB where the barrier height is not dependent on the intersite separation, the frequency exponent of $\sigma(\omega)$ is predicted to be unity and to be independent of temperature and frequency. It should be noted in passing that, even for the case of atomic tunneling, an expression similar to Eq. (8) for $\sigma(\omega)$ is obtained,[11] again with $s=1$, if the dipole moment is uncorrelated with the tunneling distance.[3]

A model for ac conduction arising from the motion of electrons between structural defects suffering a negative effective correlation energy, U_{eff}, has been developed by Elliott.[1,2] It is assumed that relaxation also occurs by HOB, but in this case the barrier height W is correlated with the intersite separation as a result of the Coulombic interaction between the charge-carrier and the charged-defect centers, $W=W_M-2e^2/\pi\epsilon\epsilon_0 R$; such a process has been termed "correlated barrier hopping," CBH.[12] The ac conductivity can be evaluated for this mechanism, and for the narrow-band limit ($\Delta_0 \ll kT$), in which all centers are degenerate and where *two* electrons are assumed to hop *simultaneously* between randomly situated D^+ and D^- centers, the result is

$$\sigma(\omega)=\frac{\pi^3}{12}N^2\epsilon\epsilon_0\omega R_\omega^6 , \tag{9}$$

where ϵ is the dielectric constant of the material, ϵ_0 that of free space, N is the concentration of pair states, and the hopping distance R_ω at a frequency ω is given by

$$R_\omega=\frac{2e^2}{\pi\epsilon\epsilon_0[W_M+kT\ln(\omega\tau_0)]} , \tag{10}$$

where W_M is the maximum barrier height (assumed to be constant for all centers). The frequency exponent for this model can be evaluated with the use of Eq. (5) and is[3]

$$s=1-\frac{6kT}{W_M+kT\ln(\omega\tau_0)} \tag{11}$$

which, to a first approximation, reduces to the simple expression[1] $s=1-6kT/W_M$. Thus, a temperature-dependent exponent is predicted, with s increasing towards unity as $T\rightarrow 0$ K, in marked contrast to the QMT or simple HOB mechanisms discussed earlier. In the broadband, i.e., low-temperature, limit ($\Delta_0 \gg kT$), N in Eq. (9) is replaced by $NkT/2\Delta_0$, where g_0' ($=N/2\Delta_0$) is the density of pair states (in $\text{eV}^{-1}\,\text{cm}^{-3}$), and so an additional T^2 temperature dependence of $\sigma(\omega)$ is introduced.[3]

It might appear that the behavior of the CBH model is also pathological in the same sense as discussed previously for the small-polaron tunneling model. In this case, however, when the *denominator* of Eq. (10) for the hopping distance tends to zero, R_ω tends to infinity. However, long before this can occur, the pair approximation breaks down, and the (dc) percolation limit is reached, with the result that the CBH model is no longer valid in any case.[2]

Several developments of this theory have been made. The assumption of randomly distributed centers used in the derivation of Eq. (9) has been relaxed for the case of melt-quenched chalcogenide glasses where pairing of charged defects may occur. The result of this is an enhancement of the frequency exponent s [Eq. (11)] by the additional factor $T/8T_g$, where T_g is the glass-transition temperature.[13]

The CBH mechanism of ac loss has also been applied to the case of materials with a mixed positive and negative U_{eff}, e.g., a-As, where both charged diamagnetic defects (D^+,D^-) and neutral, paramagnetic defects (D^0) occur together.[14] In this case, *single*-electron hopping between D^+ and D^0, or D^- and D^0, dominates the contribution of two-electron CBH between D^+ and D^- because W_M [in Eq. (10)] is considerably smaller for one-electron than for two-electron hopping. This idea has been extended[15] to the case of chalcogenide glasses, where it was proposed that at a finite temperature a small number of D^0 centers are thermally generated from D^+ and D^- centers according to the equation

$$N_0=N_\pm\exp(-U_{\text{eff}}/2kT) ,$$

and thus at high temperatures single-polaron hopping involving such thermally generated centers will dominate the ac conduction. Thus, the factor N in Eq. (9) is replaced in this case by the activated term N_0, given above, and so the ac conductivity is predicted to become much more strongly temperature dependent than at lower temperatures, where $\sigma(\omega)$ is presumed to arise from two-electron CBH amongst a fixed number of D^+ and D^- centers. Such behavior has been observed experimentally for the case of a-As_2Te_3 films.[16]

The negative temperature dependence of the frequency exponent s (widely observed in many amorphous semiconductors) arises in the CBH model because of the correlation between the barrier height and the hopping distance and the effect this has on the relaxation time. A mechanism, similar in spirit, has been proposed[3] for the case of polaron tunneling, where the (large-) polaron wells of two sites *overlap,* thereby reducing the value of the polaron hopping energy,[4,9] i.e., $W_H=W_{H0}(1-r_0/R)$, where r_0 is the polaron radius. It is assumed once again that W_{H0} is constant for all sites, whereas the intersite separation R is a random variable. The ac conductivity for this overlapping-large-polaron model has been evaluated[3] and is given by

$$\sigma(\omega)=\frac{\pi^4}{12}g_0^2(kT)^2e^2\frac{\omega R_\omega^4}{2\alpha kT+W_{H0}r_0/R_\omega^2} , \tag{12}$$

where R_ω is the hopping length at a frequency ω, determined by the quadratic equation

$$(R_\omega')^2+[\beta W_{H0}+\ln(\omega\tau_0)]R_\omega'-\beta W_{H0}r_0'=0 , \tag{13}$$

where $R_\omega'=2\alpha R_\omega$, $r_0'=2\alpha r_0$, and $\beta=1/kT$. The frequency exponent s of $\sigma(\omega)$ in this model is

$$s=1-\frac{8\alpha R_\omega+6\beta W_{H0}(r_0/R_\omega)}{2\alpha R_\omega+\beta W_{H0}(r_0/R_\omega)^2} . \tag{14}$$

It can be seen from Eq. (14) that at low temperatures the behavior of s is similar to that predicted by the CBH model, namely a linear decrease from unity, whereas at high temperatures, s tends to the limit for pure tunneling [Eq. (6)]. For values of the polaron radius r_0 such that

$r_0=(1/3\alpha)\ln(\omega\tau_0)$, s exhibits a minimum[3] at a temperature close to $0.1W_{H0}/k$. The temperature dependence of s in the overlapping-large-polaron model is shown in Fig. 1 for various values of the reduced polaron radius, $r_0'=2\alpha r_0$, and is plotted versus reduced temperature, kT/W_0, where $W_0=W_{H0}$, the polaron hopping energy. Also shown in this figure for comparison are the corresponding curves predicted for QMT of non-polaron-forming carriers [$W_{H0}=0$ in Eq. (14)] and nonoverlapping small polarons [$r_0=0$ in Eq. (14)], together with the predictions of the CBH model, again plotted against reduced temperature, where now $W_0=W_M$, the maximum barrier height.

The effect of intersite correlation effects on ac conductivity has also been considered.[3,5,8] Assuming that the interaction energy is of the form of an unscreened-Coulomb potential, it can be shown that the effect is to lower by 1 the exponent for both the temperature and the hopping distance in the expression for $\sigma(\omega)$ (for QMT and broad-band CBH), whilst the functional form for narrow-band CBH is unaltered.

The experimental data for sputtered a-P films obtained in this work will be described and discussed with reference to the models described above in the following.

II. EXPERIMENTAL

Thin films of amorphous phosphorus were prepared by rf sputtering (13.56 MHz, 60 W power) in an atmosphere of 7×10^{-3} Torr of Ar (or a 9:1 mixture of Ar and H_2) from a target of red phosphorus (2 in. diam, 0.5 in. thick), supplied by Mining and Chemical Products Electronics, Ltd. The substrate was water cooled, and a target-substrate separation of 9 cm was used.

Sandwich-geometry samples were prepared by sputtering phosphorus films onto gold electrodes, preevaporated on Corning 7059 substrates, and the samples were then transferred to a separate vacuum system for evaporation of the top electrodes. Sixteen sandwich samples, each of area 1 mm^2, were prepared on one substrate, and sample thicknesses used were between 0.5 and 3 μm.

The ac measurements were carried out using a General Radio 1621 precision capacitance bridge, which measures the equivalent parallel conductance (in the range 10^{-13}–10^{-5} Ω^{-1}) and capacitance (in the range 10^{-15}–10^{-8} F) of a sample for frequencies ($\omega/2\pi$) between 10 and 10^5 Hz, in a three-terminal arrangement (to eliminate stray capacitances). An evacuable chamber, backfilled with He at $\simeq$1 atm, was employed as a sample cell, and was inserted inside a Delta Design Environmental cabinet for control of the temperature (in the range $T=80$–470 K with a stability of $\pm\frac{1}{2}$ K).

III. RESULTS

Figure 2(a) shows the measured conductivity $\sigma_{\rm tot}(\omega)$ as a function of frequency for a 2-μm film of a-P (sputtered in argon) at various temperatures. The dc contribution is significant at low frequencies and high temperatures, whilst the frequency-dependent term dominates at high frequencies and low temperatures. The upper two curves were measured at room temperature, the uppermost being

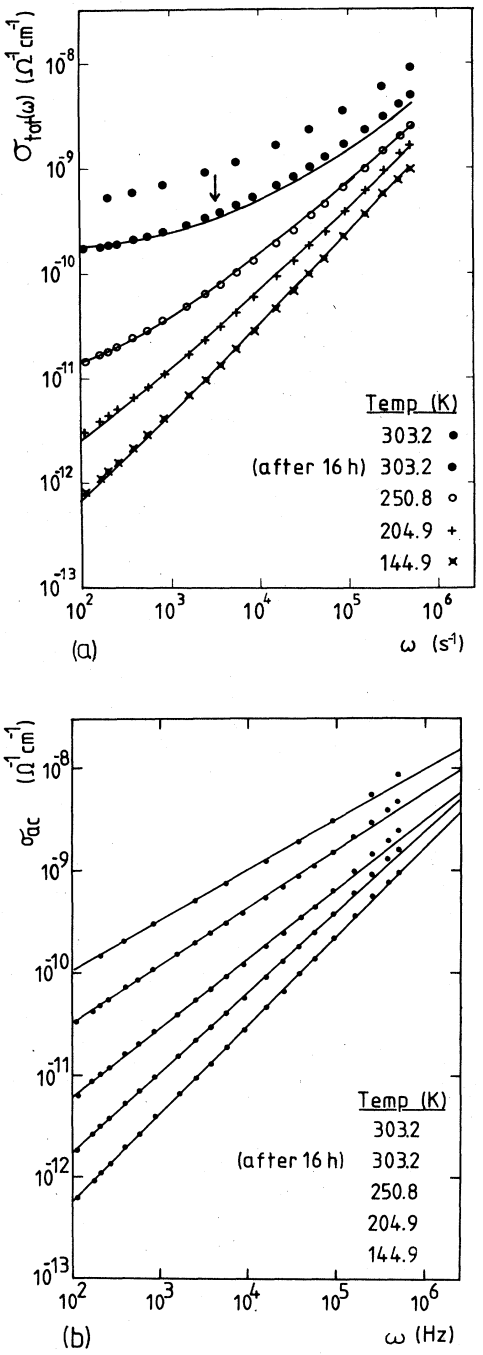

FIG. 2. (a) Total ac conductivity for an as-deposited a-P film measured at the four temperatures shown. Note the room-temperature annealing that had taken place when the sample was remeasured 16 h later. The curves in this figure are fits made using the ac conductivity calculated from the CBH model and the measured values of the dc conductivity $\sigma_{\rm dc}$ (see text for details). (b) The frequency-dependent conductivity obtained from the data shown in (a) by subtracting a frequency-independent contribution σ_0 to give a frequency exponent s which was constant and independent of frequency at each temperature. The solid lines are straight-line fits obtained by a least-squares-fitting procedure.

measured $1\frac{1}{2}$ h after deposition, whereas the lower was measured 16 h later. It is evident that some room-temperature annealing has occurred.

Subtraction of a frequency-independent contribution to the conductivity, as suggested by Eq. (2), yielded the straight lines shown in Fig. 2(b). The actual values σ_0 which were subtracted were determined by fitting $\sigma_{\rm tot}(\omega)-\sigma_0$ to the relation $\sigma_{\rm tot}(\omega)-\sigma_0=\sigma_{\rm ac}(\omega)=A\omega^s$ using a least-mean-squares-fitting program, with σ_0 as a variable parameter to obtain the best fit, and assuming that s is *constant* (at a given temperature) and independent of frequency. Values of σ_0 so obtained were in reasonable agreement ($\pm 20\%$) with the values of $\sigma_{\rm dc}$ actually measured at high temperature (see Fig. 12). However, there was considerable disagreement for lower temperatures, with $\sigma_{\rm dc}$ often being several orders of magnitude lower than σ_0.

Such a subtraction procedure, however, may be suspect for two reasons. Equation (2) assumes that $\sigma(\omega)$ and $\sigma_{\rm dc}$ arise from completely different mechanisms. However, the as-deposited (unhydrogenated) a-P films show clear evidence for variable-range hopping (i.e., a $T^{-1/4}$ temperature dependence of $\sigma_{\rm dc}$—see Fig. 12), and thus only if the hopping mechanisms were different for ac and dc conduction, or if the motion of carriers giving rise to $\sigma(\omega)$ were confined to localized regions not forming a percolation path, would the separation of terms as given by Eq. (2) be useful. Moreover, it is assumed that the frequency exponent s is independent of frequency. In fact, the theories for ac conduction which predict values for s differing from unity also predict that s should be frequency dependent [cf. Eqs. (6), (7), (11), and (14)], and clear experimental evidence for this behavior can be seen in the curvature exhibited by the lowest-temperature curve in Fig. 2(a), where the measured dc conductivity is many orders of magnitude lower than $\sigma_{\rm tot}(\omega)$ at the lowest frequency and, consequently, cannot be responsible for the curvature observed. We will return to this point later. In addition, it should be pointed out that at the lowest frequencies, i.e., those for which $\sigma(\omega)$ is the most susceptible to subtraction errors, the pair approximation will begin to break down, with the ac conductivity arising from transport within clusters rather than between pairs of sites. In such a case, of course, the relations derived in this paper based on the pair approximation, are no longer valid.

Figure 3(a) shows $\sigma_{\rm tot}(\omega)$ at the temperatures indicated for the same a-P film, but after a 1-h anneal at 140 °C. After this anneal, the temperature dependence of the dc conductivity changed in behavior from $\sigma \propto \exp(-T^{-1/4})$, characteristic of variable-range hopping, to a simple activated dependence. The magnitude of $\sigma_{\rm tot}(\omega)$ decreased by about 1 order of magnitude and the temperature dependence decreased compared with the as-deposited films. Figure 3(b), showing the frequency-dependent behavior of $\sigma_{\rm ac}(\omega)$ obtained by subtraction of σ_0, indicates that the values of s are larger and exhibit a much smaller temperature dependence than is observed for the case of as-deposited films [see Fig. 2(b)].

Figure 4(a) shows $\sigma_{\rm tot}(\omega)$ for an as-deposited (and partially annealed) film of hydrogenated amorphous phosphorus (a-P:H), prepared by sputtering in an 9:1 argon-

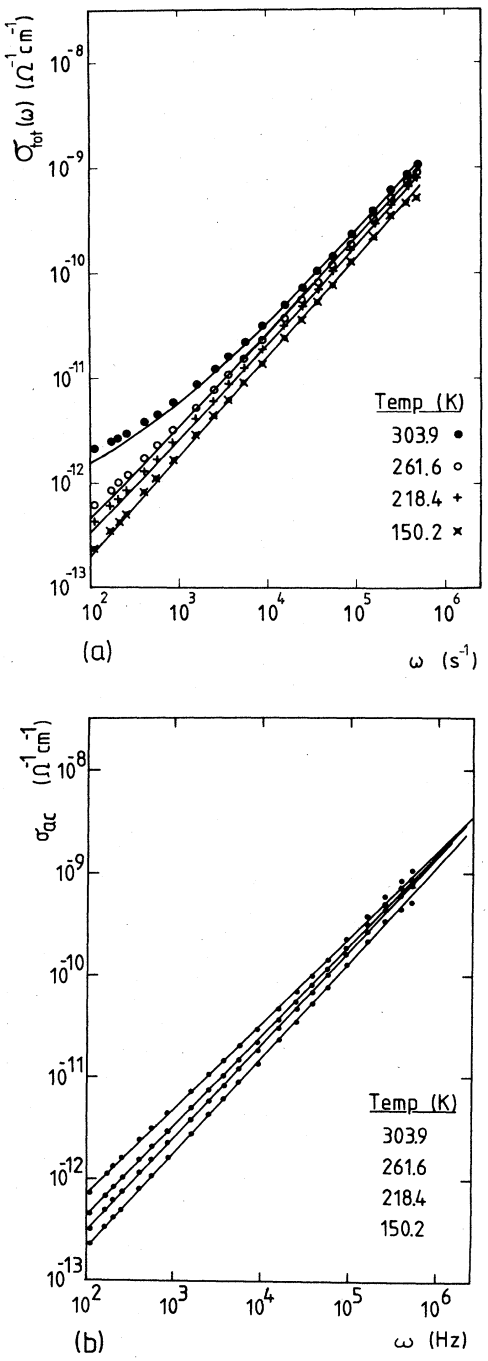

FIG. 3. (a) Total ac conductivity for an annealed a-P film (the same as for Fig. 2), measured at the four temperatures shown. The curves in this figure are fits made using the ac conductivity calculated from the CBH model and the measured values of the dc conductivity. (b) The frequency-dependent conductivity obtained from the data shown in (a) using the same fitting procedure as used in Fig. 2(b).

hydrogen atmosphere. The frequency-dependent component of the conductivity dominates the behavior, and this is in accord with the observation that a-P:H films have a lower (activated) dc conductivity and a much

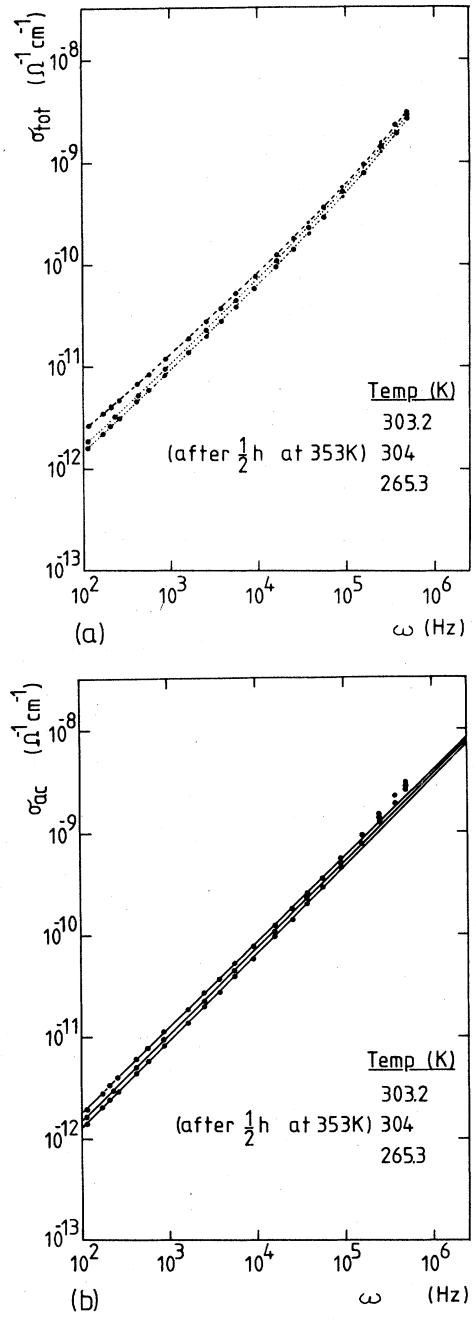

FIG. 4. (a) Total ac conductivity for an as-deposited *a*-P:H film measured at the temperatures shown. Note the partial annealing that had taken place when the sample was remeasured $\frac{1}{2}$ h later. The dashed and dotted lines are meant simply as guides for the eye and have no theoretical significance. (b) The frequency-dependent conductivity obtained from the data shown in (a) using the same fitting procedure as used in Fig. 2(b).

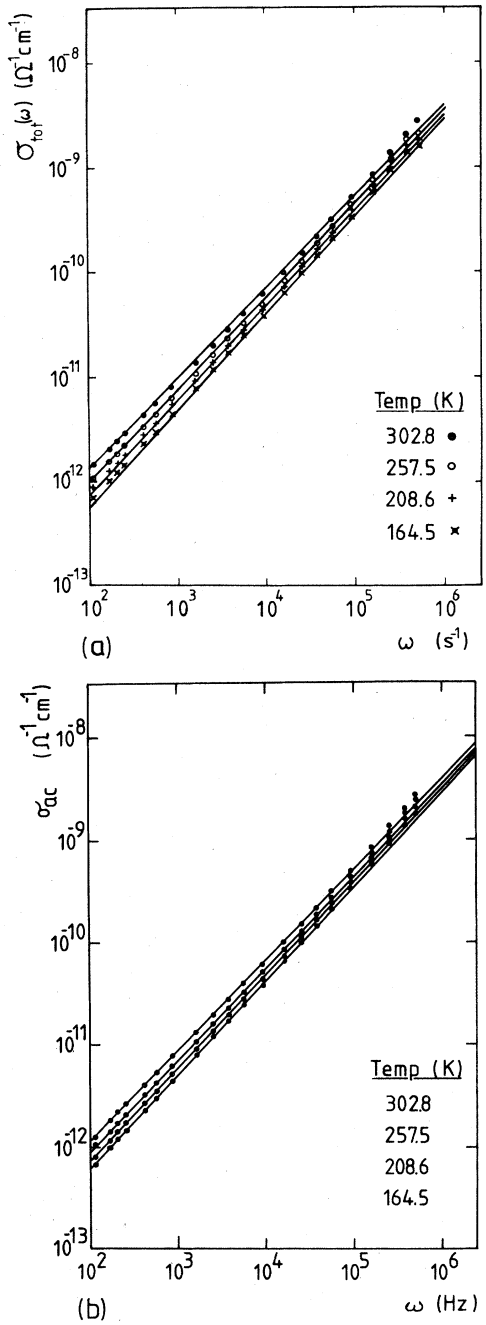

FIG. 5. (a) Total ac conductivity for an annealed *a*-P:H film measured at the four temperatures shown. The curves in this figure are fits made using the ac conductivity calculated from the CBH model (the measured values of the dc conductivity were too small to make a significant contribution). (b) The frequency-dependent conductivity obtained from the data shown in (a) using the same fitting procedure as used in Fig. 2(b).

smaller annealing effect than do pure *a*-P films. The values of s deduced from the plots of $\sigma_{ac}(\omega)$ shown in Fig. 4(b) obtained by the subtraction of σ_0 are much larger than those of pure as-deposited *a*-P films, and they exhibit a much smaller temperature dependence.

Finally, Fig. 5(a) shows $\sigma_{tot}(\omega)$ measured for this *a*-P:H film which had been annealed for 1 h at 140 °C. The magnitude of $\sigma_{tot}(\omega)$ has only changed by a factor of 2 or so (as compared with the change on annealing of more than 1 order of magnitude exhibited by as-deposited *a*-P films),

and the values of s, deduced from the curves of $\sigma_{ac}(\omega)$ obtained by subtraction of σ_0 and shown in Fig. 5(b), exhibit only a small temperature dependence.

Samples of a-P and a-P:H exhibit above 20 kHz an increase above the straight-line plots of $\sigma_{ac}(\omega)$ obtained by subtraction of σ_0 [see particularly Figs. 2(b) and 4(b)]. This could be due to contact effects,[17] where $\sigma(\omega) \propto \omega^2$ is expected at high frequencies, but, as we shall see later, this is most likely not to be entirely a spurious effect but instead a manifestation of the frequency dependence of s.

The capacitance of the samples was measured, and in the region where $\sigma_{tot}(\omega)$ is approximately proportional to ω^s, a plot of capacitance versus inverse thickness was linear; using the standard formula for a parallel-plate capacitor yields a value for the dielectric constant of a-P of $\epsilon \simeq 15$. A more detailed analysis of the capacitance data is given later (Sec. IV D).

To summarize, therefore, as-deposited films of a-P show a greater temperature dependence of the ac conductivity than is shown by either annealed or hydrogenated films, and this behavior is reflected also in the temperature dependence of the frequency exponent of the conductivity, which is shown in Fig. 6 for a variety of samples of a-P of different types. [It should be noted that the values of s shown in Fig. 6 were obtained by the subtraction procedure involving σ_0 to give constant values of s, i.e., they ignore the frequency dependence of s, particularly important for as-deposited films (see Fig. 9).]

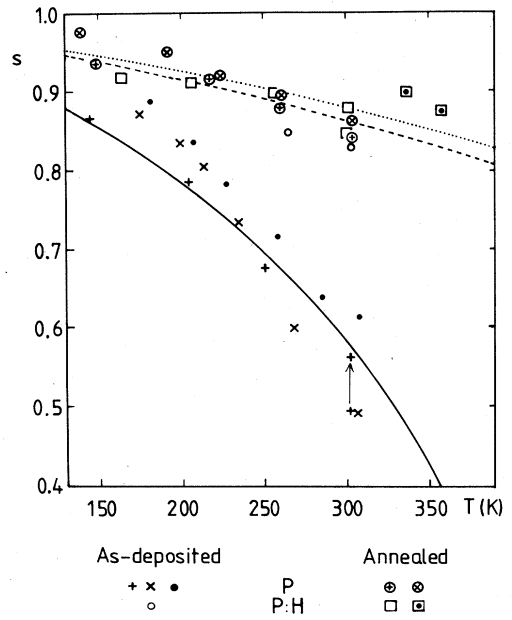

FIG. 6. Temperature dependence of the frequency exponent s for various a-P films obtained by the fitting procedure involving subtraction of a frequency-independent term σ_0, as shown in Figs. 2(b), 3(b), 4(b), and 5(b). The curves in the figure are calculated using the CBH model, with the parameters given in Table I, and assuming a fixed frequency of $\omega = 10^4$ s^{-1}. The solid curve refers to as-deposited a-P films, the dashed line to annealed a-P:H films, and the dotted line to annealed a-P films.

IV. DISCUSSION

The ac conductivity of amorphous phosphorus has not been reported previously, and its behavior upon annealing and incorporation of hydrogen is very interesting, in particular since the changes observed after such treatments are larger than those which have been observed for other amorphous semiconductors. Furthermore, the measurements reported here of the ac conductivity made over a wide range of frequencies and temperatures should, in principle, allow a conclusion to be drawn as to the likely mechanism of charge transport.

A. Quantum-mechanical tunneling model

The mechanism of quantum-mechanical tunneling has previously been applied to ac-conductivity data for many amorphous semiconductors without conspicuous success, and it turns out that the behavior of amorphous phosphorus reported here cannot be reconciled with this theory either. Perhaps the most obvious discrepancy between experiment and theory concerns the temperature dependence of s, the frequency exponent of the ac conductivity. From Eq. (6), the QMT model is seen, in its simplest form, to predict a value for s of $\simeq 0.8$ (for typical values of ω and τ_0) which is temperature *independent* (see Fig. 1). Figure 6 shows a collation of values of s (obtained by the subtraction procedure outlined previously) plotted versus temperature for many samples of a-P, both pure and hydrogenated. It can be clearly seen that the general trend is for s to decrease with increasing T, thereby conflicting with the prediction of the simple QMT model. [For QMT of nonoverlapping small polarons, a temperature dependence of s is predicted, but it is of the opposite sign—see Eq. (7) and Fig. 1.]

In addition, the wide variation in the observed values of s ($0.5 < s < 0.98$) for a-P is understandable in terms of the simple QMT model only if the characteristic relaxation time τ_0 varies by very many orders of magnitude between samples. The experimental observations are particularly difficult to reconcile with this theory for the values $s \simeq 1$ measured at lower temperatures, because this requires unrealistically small values of τ_0 ($\simeq 10^{-25}$ s). The simple QMT model also predicts that s should decrease appreciably with increasing frequency, particularly at high frequencies.[2] No such variation is observed; indeed, an increase in s with increasing frequency is observed instead [cf. Fig. 2(a)]. For these reasons, therefore, we believe that the QMT model, both for ordinary carriers and for nonoverlapping small polarons, is inappropriate as a description of our data for a-P.

B. Overlapping-large-polaron model

As discussed in the Introduction, a mechanism of QMT of large polarons, with overlapping polaron wells (OPW's),[3] predicts that $\sigma(\omega)$ should behave in some respects in a similar manner to the CBH model, namely it should have a negative temperature dependence of s, at least at low temperatures [cf. Eq. (14)]. Thus at first sight, it appears that the OPW model might be a possible candidate theory to explain our data. It can be seen by

reference to Fig. 1 that there are two distinct ways within the OPW model by which the value of s (and its temperature dependence) at a given temperature may be changed in order to account for the annealing behavior shown in Fig. 6: either the normalized polaron radius $r_0'=2\alpha r_0$ changes whilst the polaron hopping energy W_{H0} remains constant, or, alternatively, W_{H0} changes whilst r_0' remains constant. The former possibility is considered to be unlikely, since reference to Fig. 1 shows that for a fixed value of $kT/W_{H0}=0.05$ (corresponding to a value of $W_{H0}=0.52$ eV at $T=300$ K), a value of $s=0.87$ (appropriate for annealed and hydrogenated a-P films at room temperature) corresponds to $r_0'\simeq 20$, whereas $s\simeq 0.65$ (appropriate for as-deposited a-P films at room temperature) corresponds to $r_0'\simeq 2.5$. It seems improbable that annealing a sample would result in a tenfold increase in the polaron radius r_0 of a center (or, equivalently, a tenfold decrease in the spatial extent of the localized wave function, α^{-1}, or a combination of the two).

The alternative explanation in terms of a change in W_{H0} is more plausible. The curves for s as a function of r_0' shown in Fig. 1 are universal in the sense that they are plotted versus reduced temperature, kT/W_{H0}; or put another way, changes in W_{H0} result in a rescaling of the temperature axis. The annealing behavior of s can then be understood in these terms by assuming that r_0' is constant and has a value $r_0'=2.5$ (necessary to give rise to a minimum value of $s\simeq 0.65$), and that the polaron hopping energy changes from a value of $W_{H0}\simeq 0.52$ eV (i.e., $kT/W_{H0}=0.05$, giving $s=0.65$ appropriate for as-deposited a-P) to a value of $W_{H0}\simeq 1.52$ eV (i.e., $kT/W_{H0}=0.017$, giving $s=0.87$ at $T=300$ K, and corresponding to annealed or hydrogenated a-P). Thus, in this interpretation, the action of annealing (or hydrogenating) the films is to cause the polaron hopping energy to increase. Whilst again this is unlikely if the *same* center is involved before and after annealing, it is not unreasonable if annealing causes a reduction in the concentration of one type of polaron center (with a small W_{H0}) at the expense of another with a larger W_{H0}, so that there is a change in the dominant center contributing to $\sigma(\omega)$.

However, there are several features which suggest that the OPW model is unlikely to be the mechanism for ac conduction in a-P. First, no sign of a minimum is observed in the experimental plots of s versus T for a-P, as is predicted by this model for small values of r_0' (see Fig. 1).

The other feature which casts doubt on the applicability of the OPW model concerns the temperature dependence of the ac conductivity itself. Data for both as-deposited and annealed films of a-P are plotted versus reciprocal temperature in Fig. 7, from which it can be seen that, in common with other amorphous semiconductors, the temperature dependence of $\sigma(\omega)$ is much less than that of σ_{dc}, particularly at low temperatures, and is not activated in behavior. The various models described in Sec. I all predict different temperature dependences for $\sigma(\omega)$, and so, in principle, this feature ought to indicate which model (if any) best describes the data. We concentrate at present on the OPW model since we have eliminated all but this and the CBH model from consideration.

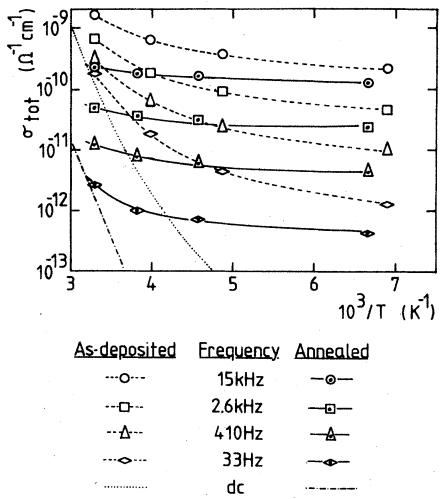

FIG. 7. Temperature dependence of the total measured ac conductivity for as-deposited and annealed a-P films at the various frequencies shown, plotted versus inverse temperature.

The temperature dependence of $\sigma(\omega)$ may, in general, be expressed in power-law form, $\sigma(\omega)\propto T^n$ (where the exponent n need not be constant), and such behavior is revealed, of course, in a $\log_{10}\sigma$ versus $\log_{10}T$ plot; the experimental data for a-P are shown in Fig. 8 plotted in this manner where, as before, $\sigma_{ac}(\omega)$ has been obtained by subtraction of σ_0. The difference in the temperature dependence of $\sigma_{ac}(\omega)$ between as-deposited and annealed samples is shown rather clearly in this figure, from which it can be seen that a T^n dependence, with n constant, does not describe the behavior of the as-deposited films. The data for the annealed films fit this relation somewhat better, with a value of $n\simeq 1$, although departures are observed at higher temperatures. On this evidence, therefore, we can dismiss the OPW model, since it predicts a considerably stronger temperature dependence in the temperature regime where the frequency exponent s is a decreasing function of temperature. The functional form of the temperature dependence of $\sigma(\omega)$ predicted by the OPW model is complicated and cannot be expressed simply as $\sigma(\omega)\propto T^n$, with n constant over a wide tempera-

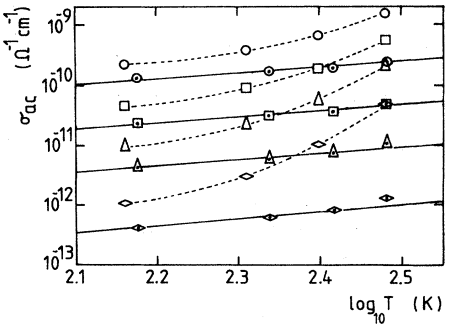

FIG. 8. Temperature dependence of the frequency-dependent conductivity obtained by the fitting procedure involving the subtraction of a frequency-independent term σ_0 plotted double logarithmically.

ture range. Nevertheless, in the region centered around $kT/W_{H0} \simeq 0.5$ (corresponding to the temperature regime shown in Fig. 8 if $W_{H0} \simeq 0.5$ eV) the hopping length R_ω has an approximately constant temperature dependence $R_\omega \sim T^{1.25}$ (for $r_0' = 2.5$), and insertion of this into Eq. (12) yields $\sigma(\omega) \sim T^6$ (for the uncorrelated case). This is obviously at variance with the much weaker dependence exhibited by the data shown in Fig. 8 and, even if the correlated form of the OPW expression is used, the dependence is predicted to decrease only to $\sigma(\omega) \sim T^4$. Thus, there is a body of evidence to support the rejection of the OPW model for the case of ac conduction in a-P.

C. Correlated-barrier-hopping model: Real part of the ac conductivity

We are left, therefore, with the correlated-barrier-hopping (CBH) model as being the only possible available contending theory for ac conduction in a-P; this model has been used in the past to account for the ac behavior of a-As, a material isostructural with and very similar in its properties to a-P.[14]

The behavior of s with T predicted by the CBH model can be analyzed in scaling terms as for the OPW model (see Fig. 1); the smaller the value of W_M, the larger the temperature dependence of s, i.e., the smaller the value of s reached at a given temperature (for a fixed value of τ_0). The annealing (or hydrogenation) behavior exhibited by a-P can therefore be explained in the framework of the CBH model in a similar manner to that discussed above for the OPW model, namely a change in the type of dominant center (having differing values of W_M) occurring on annealing or hydrogenation.

Fits to the experimental values of s as a function of temperature for a-P films made using Eq. (11) are shown in Fig. 6. The values of parameters used in calculating the curves are those given in Table I; in all cases a fixed frequency ($\omega = 10^4$ s^{-1}) has been assumed.

Although the fit appears to be reasonable over the entire temperature range measured, the agreement has to be treated with a certain degree of caution since the frequency dependence of s has been neglected in the subtraction procedure involving σ_0 used to generate $\sigma_{ac}(\omega)$, as mentioned previously. For an accurate, quantitative comparison of theory with experiment, such an approximation is not realistic (particularly when the discrepancies between the values of σ_0 obtained by fitting and σ_{dc} obtained by measurement are borne in mind). Thus, a proper fitting procedure is to fit the *total* measured ac conductivity $\sigma_{tot}(\omega)$ as a function of both frequency *and* temperature, assuming additivity of dc and ac conductivities [Eq. (2)], but using the measured value of σ_{dc}, rather than σ_0, as the frequency-independent contribution.

We show in Fig. 2(a) the total ac conductivity $\sigma_{tot}(\omega)$ for as-deposited a-P films fitted using the *measured* values of σ_{dc},[18] and using W_M and τ_0 as variable parameters in the CBH model, scaling the calculated curves so as to fit the value of $\sigma_{tot}(\omega)$ at $\omega = 10^5$ s^{-1} for the lowest temperature (i.e., thereby effectively fixing N). The values obtained by fitting were $W_M = 0.7$ eV and $\tau_0 = 3 \times 10^{-10}$ s. Only by choosing such a relatively large value of τ_0 could the pronounced frequency dependence of the frequency exponent s be reproduced. This behavior is shown more clearly in Fig. 9, where the ac conductivity $\sigma_{ac}(\omega)$ predicted by the CBH model is plotted using the above values for W_M and τ_0; the curvature exhibited by these plots, it must be stressed, is *not* influenced by the dc conductivity and comes about solely through the frequency dependence of s predicted by the CBH model, an effect particularly pronounced when W_M is small. The danger of assuming that the frequency exponent is independent of frequency, as in Figs. 2(b), 3(b), 4(b), and 5(b), is therefore self-evident. The departures from the fit for the room-temperature data could be due to further annealing taking place during the course of the measurements—recall that the theoretical curves have been fitted to the lowest-temperature data, not the room-temperature data—or to contact effects at high frequency.

The fits of the CBH model to the $\sigma_{tot}(\omega)$ data for annealed a-P, again using measured values for σ_{dc}, are shown in Fig. 3(a); the parameters determined using this fit are $W_M = 1.6$ eV and $\tau_0 = 5 \times 10^{-10}$ s. The much larger value of W_M ensures both that the frequency dependence (i.e., s) is greater at a given temperature and also that the temperature dependence of $\sigma(\omega)$ is less than for the as-deposited films.

Finally, we show in Fig. 5(a) the fits to the $\sigma_{tot}(\omega)$ data for annealed a-P:H films. The fits are somewhat less good than the two previous examples (due possibly either to contact effects in the experimental data at high frequencies or the presence of a nonrandom distribution of centers which is not taken into account in the model fits); the parameters obtained from the fit are $W_M = 1.4$ eV and $\tau_0 = 5 \times 10^{-9}$ s.

The various values for W_M and τ_0 obtained from the fitting of the CBH model to the $\sigma(\omega)$ data for the various types of amorphous phosphorus films studied in this work are collected together for convenience in Table I.

In conclusion, the very good agreement shown between experimental data and the curves calculated for the CBH model using Eq. (9) indicate that, at least for temperatures above 150 K, the narrow-band limit ($2\Delta_0 < kT$) is obeyed,

TABLE I. Parameters for various forms of amorphous phosphorus relating to ac conductivity (obtained by fitting using the CBH model) and dc conductivity.

	W_M (eV)	τ_0 (s)	N (cm^{-3})	ϵ_∞	E_0 (eV)
As-deposited a-P	0.70	3×10^{-10}	1.4×10^{20}[a]	15.8	
Annealed a-P	1.6	5×10^{-10}	1.3×10^{20}	14.7	1.0–1.05
Annealed a-P:H	1.4	5×10^{-9}	2.4×10^{20}	18.1	1.2–1.25

[a]Assuming the concentrations of singly and doubly occupied states are equal, $N_1 = N_2$.

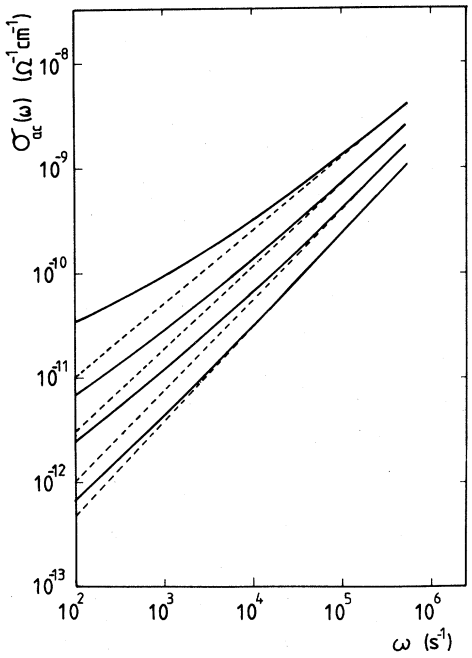

FIG. 9. The frequency-dependent conductivity calculated for the CBH model using the parameters appropriate for as-deposited a-P, and as used in Fig. 2(a). The solid lines are the calculated curves; the dashed lines are straight lines drawn as tangents to the high-frequency parts and are intended to emphasize the curvature exhibited by the plots of $\sigma_{ac}(\omega)$. (Note that the dc component is *not* included in these plots.)

i.e., $\Delta_0 < 6.5$ meV; no evidence for the much stronger temperature dependence associated with the broadband limit is discernible in the present data. The values for the characteristic relaxation time τ_0 obtained from the fitting procedures described previously and given in Table I lie in the region $\tau_0 \simeq 10^{-10}$ s. Such values are higher than those which would be expected for typical inverse phonon frequencies, although such a discrepancy is not unexpected when lattice-relaxation effects are important, as we believe to be the case here.

D. Correlated-barrier-hopping model: Imaginary part of the ac conductivity

Thus far in this paper, we have concentrated exclusively on the real part of the ac conductivity, denoted henceforth by $\sigma_1(\omega)$, neglecting the imaginary part of the conductivity $[\sigma_2(\omega)]$, which is related to the dielectric constant. Indeed, this is the approach adopted in very many papers dealing with frequency-dependent electrical transport in amorphous semiconductors. However, valuable information can be lost if $\sigma_2(\omega)$ is neglected; in particular, models for ac conduction also make specific predictions concerning the dielectric constant, and comparison of theory and experiment is straightforward since capacitance measurements are inherently much more accurate than conductance measurements when made using a conventional bridge. Although the real and imaginary parts of the conductivity are related via the Kramers-Kronig relations, and as such the imaginary part would appear to carry no more information than is contained within the real part, nevertheless, if the frequency exponent s, of $\sigma_1(\omega)$ is itself frequency dependent, extraction via the Kramers-Kronig relations of $\sigma_2(\omega)$ is imprecise for data taken only over a limited frequency range. In such cases, capacitance and conductance measurements, analyzed together as a function of frequency and temperature, set a severe test for any model of the process involved.

The total measured capacitance $C_{\rm tot}(\omega)$, like the conductance, can be decomposed into two components, a dispersive term $C(\omega)$ and a nondispersive term C_∞, viz.,

$$C_{\rm tot}(\omega) = C(\omega) + C_\infty \ . \tag{15}$$

These two components arise from different processes, C_∞ being due to high-frequency atomic and dipolar vibrational transitions, whereas $C(\omega)$ is determined by the loss mechanisms under consideration in this paper. Several methods of eliminating the nondispersive component exist, e.g., measurement at high frequencies [where $C_{\rm tot}(\omega) \rightarrow C_\infty$], adjustment of C_∞ until the resulting $C(\omega)$ obeys a power-law dependence, or numerical differentiation of the capacitance data, whereupon the constant terms involving C_∞ drop out. Thus, if the dispersive part of the capacitance obeys the power law

$$C(\omega) \sim \omega^{s'-1} \tag{16}$$

(where s' is *not* equal to s, the frequency exponent for the real part of the conductivity), a plot of $\log_{10}[-dC/d(\ln\omega)]$ versus $\log_{10}\omega$ should yield a straight line of slope $s'-1$. This differentiation technique has been used in the present work since the measured change of capacitance with frequency is often small (e.g., a $\sim 1\%$ change in C for four decades variation in ω for the annealed a-P films). Figure 10 shows capacitance data for an annealed a-P film (the same as for Fig. 3) at two temperatures where $-dC/d(\ln\omega)$ is plotted versus frequency; also shown in each part of the figure are the measured values of $C_{\rm tot}(\omega)$ and the values for $C(\omega)$ resulting from subtraction of C_∞. Note that the plots of $-dC/d(\ln\omega)$ and $C(\omega)$ have the same gradient, as they should, and that the slope $s'-1$ decreases as the temperature decreases (i.e., s' and s behave in a qualitatively similar manner). Values for ϵ_∞, derived from C_∞ obtained in this way for various types of films, are given in Table I.

It has been shown[3] that the ratio of the imaginary and real parts of the conductivity, related to the frequency-dependent capacitance and conductance by

$$\frac{\sigma_2(\omega)}{\sigma_1(\omega)} = \frac{\omega C(\omega)}{G(\omega)} \ , \tag{17}$$

has a characteristically different functional form for the various mechanisms of dielectric relaxation. Thus, for simple QMT,

$$\frac{\sigma_2}{\sigma_1} = -\frac{2}{5\pi}\ln(\omega\tau_0) \ , \tag{18}$$

and for CBH, to a first approximation (for small kT/W_M),

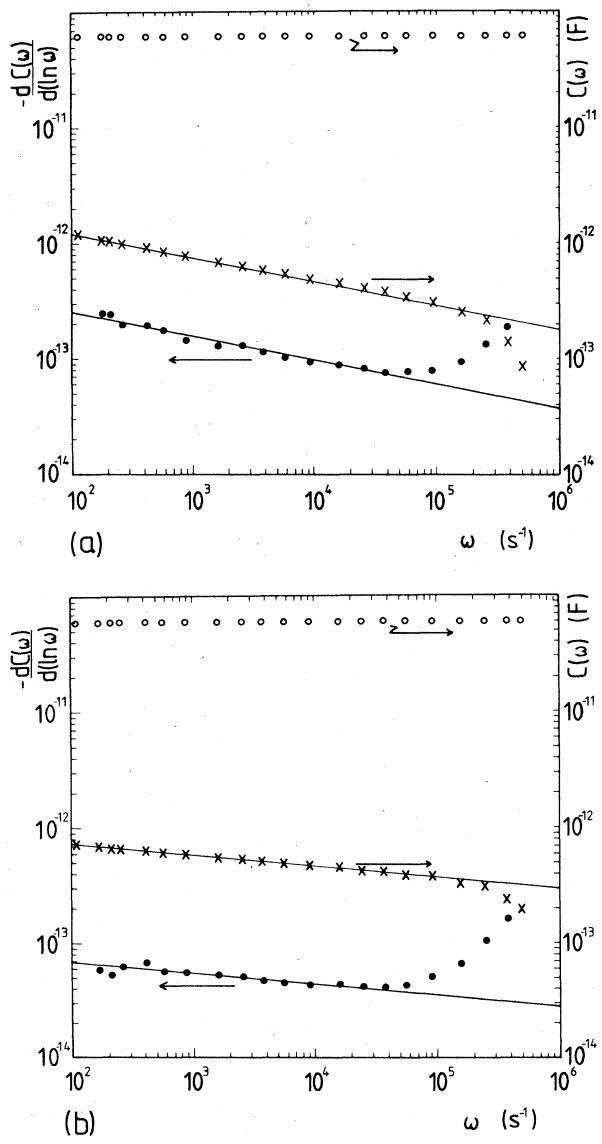

FIG. 10. Capacitance data for an annealed a-P film (the same as for Fig. 3). The total measured capacitance data are represented by open circles, the frequency-dependent contribution by the crosses, and the numerical differential of the data, $-dC/d(\ln\omega)$, is shown by the solid circles in each case for (a) $T=303.9$ K and (b) $T=150.2$ K.

$$\frac{\sigma_2}{\sigma_1}=-\frac{2\ln(\omega\tau_0)}{\pi}\left[1+\frac{3kT}{W_M}\ln(\omega\tau_0)\right]. \tag{19}$$

Note that Eq. (19) predicts a temperature dependence for σ_2/σ_1, whereas Eq. (18) does not. (An expression for σ_2/σ_1 for the OPW model has not been given and, although it is expected to be temperature dependent, we have already excluded this model and do not consider it further.)

We show in Fig. 11 the experimental data of σ_2/σ_1 plotted versus the logarithm of the frequency for an annealed a-P film at two temperatures. Note that σ_2/σ_1 is

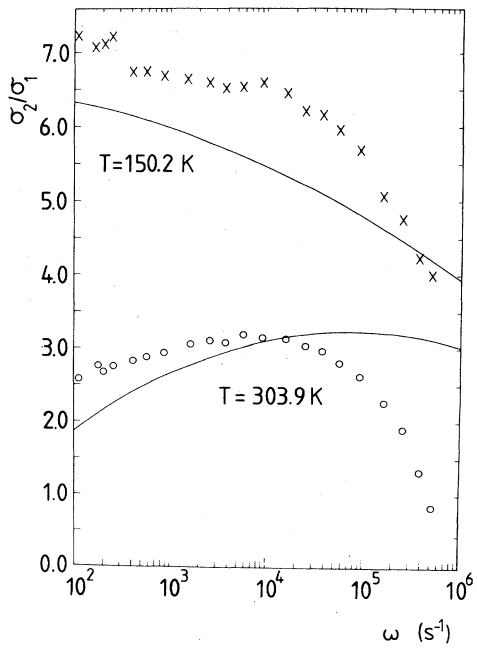

FIG. 11. Ratio of the imaginary and real parts of the ac conductivity, $\sigma_2/\sigma_1=\omega C(\omega)/G(\omega)$, for an annealed a-P film at two temperatures, $T=150.2$ K (crosses) and $T=303.9$ K (open circles). The curves represent the behavior of σ_2/σ_1 predicted by the CBH model.

observed to be temperature dependent and, moreover, the shape of the σ_2/σ_1 plots is qualitatively different at the two temperatures. Also shown in the figure are the curves corresponding to the prediction of the CBH model [i.e., Eq. (19)], using the same values of the parameters W_M and τ_0 already deduced from the fitting of the real part of the conductivity [Fig. 3(a)] and given in Table I. The fit between theory and experiment is regarded as good, bearing in mind that no extra variable parameters are used in the calculation of σ_2/σ_1. The qualitative behavior of the frequency and temperature dependence of σ_2/σ_1 is reproduced by the CBH model, and the magnitude is correct to within 10% (except for the very-high-frequency region for the high-temperature data); the calculated curve does, in fact, decrease to the value reached experimentally at $\omega=5\times10^5$ s^{-1} at a higher frequency of $\omega=5\times10^8$ s^{-1}. This discrepancy is ascribed to the fact that Eq. (19) is only approximate; higher-order terms become important at high temperatures and/or high frequencies, which would accelerate the rate of decrease of σ_2/σ_1 in the high-frequency region and so bring theory and experiment more into agreement. [In addition, the errors in $C(\omega)$ increase at high frequencies, where $C(\omega)\rightarrow C_\infty$.] It should be noted in passing that the fits to σ_2/σ_1 are very sensitive to the values of the parameters used (particularly so for τ_0), and are *more* sensitive than the fits made to just the real part of the ac conductivity.

E. Nature of the defect states

The fits to the ac-conductivity data made using the CBH model and discussed above indicate that the max-

imum barrier height W_M differs by a factor of approximately 2 between as-deposited and annealed states of unhydrogenated a-P films (see Table I). This behavior can be understood if, as mentioned earlier, different centers are involved in each case. In particular, we postulate that in the as-deposited state, a-P films contain a significant concentration of paramagnetic centers associated with dangling bonds containing a single, unpaired electron (P_2^0), giving rise to a deep gap state. Annealing the samples causes these centers to recombine or reconstruct, thereby giving, respectively, either perfectly bonded atoms (P_3^0), which, of course, do not give rise to gap states, or diamagnetic spin-paired charge defects (e.g., P_4^+,P_2^-) suffering a negative effective correlation energy U_{eff},[19] which do give rise to gap states, but not at the same energy as those associated with P_2^0. Evidence for the effect of annealing on the defect states comes from studies of the dc conductivity in a-P films. As-deposited films exhibit clear evidence for variable-range-hopping dc conduction, i.e.,

$$\sigma_{\text{dc}}=\sigma_0\exp[(-T_0/T)^{1/4}]$$

(see Fig. 12); the densities of states deduced from the slopes of the $\ln\sigma_{\text{dc}}$-versus-$T^{-1/4}$ plots shown in Fig. 12(b) using the equation[9]

$$T_0=\frac{16\alpha^3}{kN(E_F)} \tag{20}$$

is $N(E_F)\simeq(2-3)\times10^{18}$ $\text{eV}^{-1}\text{cm}^{-3}$ (assuming that the midgap electron states associated with defects are strongly localized with a radius of the localized wave function of $\alpha^{-1}=2.5$ Å). Annealing the as-deposited films removes this behavior and a simple activated temperature dependence is then exhibited, $\sigma_{\text{dc}}=\sigma_0'\exp(-E_0/kT)$; values for the activation energy E_0 for annealed unhydrogenated and hydrogenated a-P films are also given in Table I.

The changes observed in the ac-conductivity behavior of a-P films on annealing are then explicable in a manner similar to that employed previously for the case of a-As;[14] namely, that in the as-deposited state, *one*-electron CBH occurs between P_2^0 and P_4^+ (or P_2^-) centers, with the maximum barrier height for this process being $W_{M_1}=0.7$ eV, whereas in the annealed state, *two*-electron CBH between P_4^+ and P_2^- centers is dominant, for which $W_{M_2}=1.6$ eV.

W_{M_1} is expected to be less than W_{M_2} because it obviously takes less energy to excite one electron out of a P_2^- site than it does to excite two electrons. The magnitude of W_{M_1} cannot be ascertained independently since the relative positions of the defect levels within the gap are not known for the case of a-P.

However, for the case of the annealed films, where it is presumed that only diamagnetic, charged defects are present, an independent estimate for W_2 can be made. The energy W_2 is simply the energy required to remove two electrons from a P_2^- center, thereby forming a P_4^+ center. If this interconversion takes place *indirectly* by means of excitation to the conduction band, then an estimate for W_M is simply

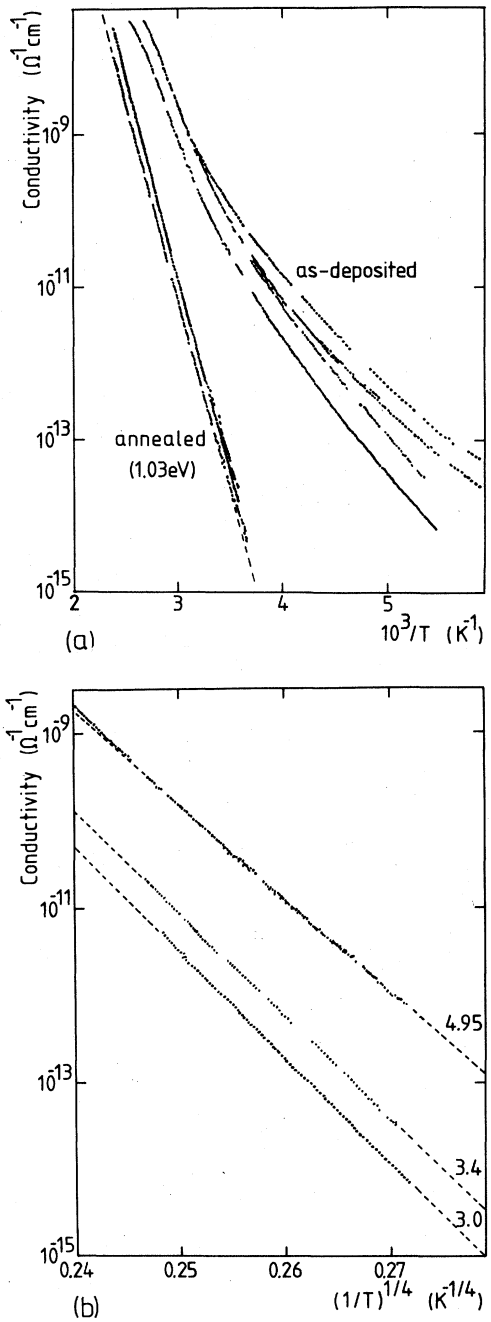

FIG. 12. dc-conductivity data for various forms of a-P films. (a) σ_{dc} for as-deposited and annealed a-P films, plotted versus inverse temperature. (b) σ_{dc} for as-deposited a-P films plotted versus $T^{-1/4}$.

$$W_M=2(E_A-E_F)\,, \tag{21}$$

where E_A-E_F is the energy separation between the Fermi level and the conduction-band edge at E_A, and is the *average* energy per electron required to take an electron from the highest-lying occupied state (P_2^-) and place it in the conduction band. A value for the energy separation between the mobility edge at E_C and E_F at a temperature T

can be obtained from the measured dc-conductivity activation energy E_0,

$$E_C - E_F \simeq E_0 - \gamma T \ , \tag{22}$$

where γ is the (linear) temperature coefficient for this energy separation, approximately equal to *half* the temperature coefficient β for the optical band gap (if it is assumed that E_F lies roughly at midgap). Values for β are 1.65×10^{-4} eV K^{-1} for both as-deposited and annealed pure a-P films and 1.4×10^{-4} eV K^{-1} for a-P:H films.[18] Thus from Eq. (21), $E_C - E_F \sim 0.95$—1.0 eV is obtained for annealed a-P films; if it is further assumed that the width of the tail states in a-P is $E_C - E_A \simeq 0.2$ eV, not an unreasonable value, then $E_A - E_F$ becomes equal to 0.75—0.8 eV and hence, from Eq. (20), W_M is predicted to lie in the range 1.5—1.6 eV, in good agreement with the value $W_M = 1.6$ eV obtained from fitting the ac data. Similar arguments for the case of annealed a-P:H films, assuming bipolaron CBH to be dominant, give an estimated value for W_M in the range 1.9—2.0 eV, higher than that found by fitting (1.4 eV). This discrepancy could be partly due to a larger tail-state width existing in a-P:H than the postulated value of 0.2 eV, although this cannot account for all the difference.

Another interpretation of the $W_M = 1.4$ eV value found by fitting could be that it is associated with a *single*-electron CBH process. However, in this case it is difficult to understand why W_M should increase by a factor of 2 relative to as-deposited a-P when the optical gap increases only from 1.72 to 1.88 eV on hydrogenation (see later). Thus, we are at a loss to explain the behavior brought about by hydrogenation, unless hydrogen-related states are introduced into the gap, at a position unrelated to those for native defects.

If it is accepted that the above procedure is valid and that the defects in annealed a-P do suffer a negative U_{eff}, the value of W_M obtained by fitting the ac data for as-deposited a-P can be interpreted, if not independently estimated. For single-electron CBH, the process which will, in general, be dominant will be that which has the smallest value of W_M [cf. Eqs. (9) and (10)], and for a center suffering a negative U_{eff}, such as P_2^-, the first electron takes more energy to remove than the second.[20] Thus, we identify the value $W_M = 0.7$ eV obtained from the fits to the ac data for as-deposited a-P as the energy to remove the second electron; i.e., the process $P_4^0 \rightarrow P_4^+$ is deemed to be the dominant relaxation mechanism. The energy required for the other process, namely $P_2^- \rightarrow P_4^0$, is therefore simply $1.6 - 0.7 = 0.9$ eV.

Finally in this section, we address the matter of the concentrations of the defects obtained from the ac measurements and those obtained from other studies. In the present context, estimates for the defect concentration may be obtained from three experiments, ac conductivity, dc conductivity exhibiting an $\exp(-T^{-1/4})$ temperature dependence, and electron-spin resonance (ESR). Values of N for a-P obtained from the fitting of the CBH model, given in Table I, are of the order $N \sim 1\times10^{20}$ cm^{-3}, the density of states obtained from measurements of σ_{dc} of as-deposited a-P is $N(E_F) \sim 3\times10^{18}$ eV^{-1} cm^{-3} (assuming $\alpha^{-1} = 2.5$ Å), and the value obtained from ESR measurements[21] on *bulk* red a-P (*not* thin films as studied here) is $N \sim 10^{17}$ cm^{-3}. Note that ESR is sensitive only to paramagnetic centers, and, in addition, that the density of such centers might well be considerably higher in the a-P films studied here (particularly in the as-deposited state) than the estimate for the bulk material might indicate. Furthermore, in evaluating the defect concentration for all three techniques it is implicitly assumed that the concentration of defects is *uniform* throughout the volume of the material, although this might well not be the case in practice if, for example, the defects are concentrated at void surfaces. In such a case of nonuniform distribution, ac and dc conductivities would *not* be expected to yield similar results, since ac loss could take place by relaxation of the centers at the void surfaces, whereas such defect states would not constitute a percolation path through the sample, a requirement for a hopping contribution to the dc conductivity. [Bulk red a-P (Mining and Chemical Products) has a spherulite growth morphology[22] for which a nonuniform distribution of states might be likely; however, this material proved too resistive for ac measurements to be performed.]

Nevertheless, the values of N obtained from the CBH theory appear perhaps rather high, particularly for the case of as-deposited a-P, where a value for the product of concentrations of P_2^0 (N_1) and P_4^+ (N_2) centers, $N_1 N_2 \simeq 2\times10^{40}$ cm^{-6}, is obtained. Insertion of $N_1 \sim 10^{17}$ cm^{-3}, derived from the ESR results on *bulk* a-P,[21] gives a physically unrealistic estimate of $N_2 \sim 1.4\times10^{23}$ cm^{-3}. This problem is alleviated to a certain extent should N_1 be higher; the value given in Table I is calculated assuming $N_1 = N_2$. Whilst similar high defect concentrations are not unknown in as-deposited films of amorphous semiconductors (e.g., Si or Ge), there is no available experimental (ESR) evidence for a-P thin films with which to carry the discussion further.

Mention should be made of the relative concentrations of defect centers found for the various forms of a-P studied in this work as estimated by fitting the CBH model to the ac data. If the assumption is made that $N_1 \simeq N_2$ for the as-deposited a-P films, then it can be seen from Table I that the densities for as-deposited and annealed films of unhydrogenated a-P are very similar. This is understandable if the action of annealing is simply to transform all paramagnetic P_2^0 centers into diamagnetic charged centers, P_4^+,P_2^-, whereupon only bipolaron CBH remains as a relaxation mechanism, and as a consequence the effective maximum barrier height W_M rises from 0.7 eV, characteristic of single-polaron CBH, to 1.6 eV, characteristic of bipolaron CBH in a-P.

What, then, is expected to be the effect of incorporation of hydrogen in the a-P films? Two consequences might be expected: the hydrogen might be expected to saturate any paramagnetic centers present (especially after subsequent annealing); in addition, the states at the band edges might be eroded as a consequence of the formation of P—H bonds (giving rise to states deep within the valence band) at the expense of the weak P—P bonds responsible for the tail states, thereby increasing the size of the gap, as observed in a-Si:H.[23] The latter behavior is indeed observed; the optical gap [as deduced from the extrapolation

of plots of $(\alpha\hbar\omega)^{1/2}$ versus $\hbar\omega$] is measured to be 1.72 eV at room temperature for *a*-P (in *both* as-deposited and annealed states), whereas for hydrogenated material, *a*-P:H, the gap is 1.88 eV at the same temperature (again irrespective of annealing). Thus, on this basis, and if the same (native) defects are responsible for the ac conduction as in annealed *a*-P, it would be expected that $\sigma(\omega)$ should decrease on hydrogenation (if the defect levels are pinned to the band edges and track with them and if N is the same in both cases). However, it is found experimentally that $\sigma(\omega)$ for annealed *a*-P:H at a given temperature and frequency is approximately twice as large as that for annealed *a*-P at the same temperature and frequency (see figs. 3 and 5). Moreover, the slope s for *a*-P:H at the lowest temperature is less than that for *a*-P, consistent with the smaller value of W_M found by fitting. Thus, hydrogenation seems to introduce *more* active states into the gap which can contribute to the ac conduction. It is difficult to speculate as to the likely nature of such states and their mode of formation, but incorporated H_2O may perhaps be responsible. It should be stressed, however, that the ac behavior of the hydrogenated material, like its unhydrogenated counterpart, seems to be accounted for by the CBH model.

V. CONCLUSIONS

The real and imaginary parts of the ac conductivity as well as the dc conductivity, of thin films of amorphous phosphorus (*a*-P), prepared by rf sputtering, have been measured for the first time in the frequency range 10^2—10^6 s^{-1} and in the temperature range 150—300 K.

As-deposited *a*-P films exhibit an ac conductivity $[\sigma(\omega)]$ whose magnitude is rather strongly temperature dependent and whose frequency exponent s is also markedly temperature dependent. The dc conductivity of such films exhibits an $\exp(-T^{-1/4})$ temperature dependence characteristic of variable-range hopping. Annealing such films causes the temperature dependence of both $\sigma(\omega)$ and s to become much weaker (and the dc conductivity to become activated); introducing hydrogen during the deposition process has qualitatively the same effect.

Of the various models for ac conduction in amorphous semiconductors that have been proposed in the literature, only one, the correlated-barrier-hopping (CBH) model,[1] is consistent with all aspects of the loss data. Fits using this model are in good agreement with the experimental data for all temperatures and frequencies measured. Estimates for the concentration of defects responsible are of the order $N \sim 10^{20}$ cm^{-3}.

The very large effect that annealing has on the transport properties of unhydrogenated *a*-P is ascribed to the removal of paramagnetic, neutral defect states (P_2^0) by thermal treatment. The ac conductivity of as-deposited *a*-P films is then ascribed to one-electron CBH between P_2^0 and P_4^+ centers, and that for annealed films to two-electron CBH between P_2^- and P_4^+ centers.

Hydrogenation of *a*-P films causes the optical gap to increase and it would be expected, therefore, that the maximum barrier height, W_M, associated with the CBH process would increase concomitantly. In fact, the fits to the experimental data indicate that W_M *decreases;* the cause of this surprising change is not understood, but it is surmised that hydrogen-related states in the gap might be responsible.

Finally, it should be remarked that a proper test for any model of ac loss in amorphous semiconductors is to compare with experiment for both real (σ_1) and imaginary (σ_2) parts of the conductivity (i.e., conductance and capacitance) as a function of both frequency and temperature. In particular, fits to σ_2/σ_1 are much more sensitive than to σ_1 alone.

---

*Present address: Lucas Research, Solihull, West Midlands, UK.

†Present address: Department of Physics, University of Leicester, Leicester, UK.

[1]S. R. Elliott, Philos. Mag. **36**, 1291 (1977).

[2]S. R. Elliott, Adv. Phys. (to be published).

[3]A. R. Long, Adv. Phys. **31**, 553 (1982).

[4]I. G. Austin and N. F. Mott, Adv. Phys. **19**, 41 (1969).

[5]M. Pollak, Philos. Mag. **23**, 519 (1971).

[6]H. Böttger and V. V. Bryskin, Phys. Status Solidi B **78**, 415 (1976).

[7]P. N. Butcher and K. J. Hayden, in *Proceedings of the Seventh International Conference on Amorphous and Liquid Semiconductors,* edited by W. E. Spear (Centre for Industrial Consultancy and Liaison, University of Edinburgh, Edinburgh, 1977), p. 234.

[8]A. L. Efros, Philos. Mag. B **43**, 829 (1981).

[9]M. Pollak, Phys. Rev. **138**, A1822 (1965).

[10]M. Pollak and G. E. Pike, Phys. Rev. Lett. **28**, 1449 (1972).

[11]G. Frossati, R. Maynard, R. Rammal, and D. Thoulouze, J. Phys. (Paris) Lett. **38**, L153 (1977).

[12]S. R. Elliott, Philos. Mag. B **37**, 553 (1978).

[13]S. R. Elliott, Philos. Mag. B **40**, 507 (1979); J. Non-Cryst. Solids **35-36**, 855 (1980).

[14]G. N. Greaves, S. R. Elliott, and E. A. Davis, Adv. Phys. **28**, 49 (1979).

[15]K. Shimakawa, J. Phys. (Paris) Colloq. **42**, C4-167 (1981); Philos. Mag. B **46**, 123 (1982).

[16]H. K. Rockstad, Solid State Commun. **9**, 2233 (1971); J. Non-Cryst. Solids **8-10**, 621 (1972).

[17]R. A. Street, G. R. Davies, and A. D. Yoffe, J. Non-Cryst. Solids **5**, 276 (1971).

[18]P. Extance, Ph.D. thesis, University of Cambridge, 1983 (unpublished).

[19]P. W. Anderson, Phys. Rev. Lett. **34**, 953 (1975).

[20]N. F. Mott, E. A. Davis, and R. A. Street, Philos. Mag. **32**, 961 (1975).

[21]B. V. Shanabrook, S. G. Bishop, and P. C. Taylor, J. Phys. (Paris) Colloq. **42**, C4-865 (1981).

[22]P. Extance and S. R. Elliott, Philos. Mag. B **43**, 469 (1981).

[23]B. Von Roedern, L. Ley, M. Cardona, and F. W. Smith, Philos. Mag. B **40**, 433 (1979).